2015

Nano-bioelectronics via dip-pen nanolithography

Cathal O'Connell
University of Wollongong, cathal@uow.edu.au

Michael J. Higgins
University of Wollongong, mhiggins@uow.edu.au

Simon E. Moulton
University of Wollongong, smoulton@uow.edu.au

Gordon G. Wallace
University of Wollongong, gwallace@uow.edu.au

Publication Details

O'Connell, C. D., Higgins, M. J., Moulton, S. E. & Wallace, G. G. (2015). Nano-bioelectronics via dip-pen nanolithography. Journal of Materials Chemistry C, 3 (25), 6431-6444.

Nano-bioelectronics via dip-pen nanolithography

Abstract
The emerging field of nano-biology is borne from advances in our ability to control the structure of materials on finer and finer length-scales, coupled with an increased appreciation of the sensitivity of living cells to nanoscale topographical, chemical and mechanical cues. As we envisage and prototype nanostructured bioelectronic devices there is a crucial need to understand how cells feel and respond to nanoscale materials, particularly as material properties (surface energy, conductivity etc.) can be very different at the nanoscale than at the bulk. However, the patterning of organic bioelectronic materials is often not achievable using conventional fabrication techniques, especially on soft, biocompatible substrates. Nonconventional nanofabrication strategies are required. Dip-pen nanolithography is a nanofabrication technique which uses the nanoscale tip of an atomic force microscope to direct-write functional inks. Over the past decade, the technique has evolved as uniquely capable in the realm of bio-nanofabrication, with the capability to deposit both biomolecules and electrode materials. This review highlights this new tool for fabricating nanoscale bioelectronic devices, and for enabling heretofore unrealised experiments in the response of living cells to tailored nano-environments. We firstly introduce bioelectronics, followed by a survey of different lithography methods and their use to achieve paradigmic bioelectronic architectures. We then focus on dip-pen nanolithography, highlighting the range of bioelectronic materials and biomolecules which can be deposited using the technique, as well as its demonstrated use as a lithography tool in nano-biology. We discuss the progress made towards upscaling the DPN technology towards larger areas, in particular via the polymer pen approach.

Keywords
via, bioelectronics, dip, nano, pen, nanolithography

Disciplines
Engineering | Physical Sciences and Mathematics

Publication Details
O'Connell, C. D., Higgins, M. J., Moulton, S. E. & Wallace, G. G. (2015). Nano-bioelectronics via dip-pen nanolithography. Journal of Materials Chemistry C, 3 (25), 6431-6444.

ARTICLE

Nano-bioelectronics via dip-pen nanolithography

Cite this: DOI: 10.1039/xoxxoooooox

C.D. O'Connell, M.J. Higgins, S.E. Moulton and G.G. Wallace*

Received ooth January 2012,
Accepted ooth January 2012

DOI: 10.1039/xoxxoooooox

The emerging field of nano-biology is borne from advances in our ability to control the structure of materials on finer and finer length-scales, coupled with an increased appreciation of the sensitivity of living cells to nanoscale topographical, chemical and mechanical cues. As we envisage and prototype nanostructured bioelectronic devices there is a crucial need to understand how cells feel and respond to nanoscale materials, particularly as material properties (surface energy, conductivity etc.) can be very different at the nanoscale than at the bulk. However, the patterning of organic bioelectronic materials is often not achievable using conventional fabrication techniques, especially on soft, biocompatible substrates. Nonconventional nanofabrication strategies are required. Dip-pen nanolithography is a nanofabrication technique which uses the nanoscale tip of an atomic force microscope to direct-write functional inks. Over the past decade, the technique has evolved as uniquely capable in the realm of bio-nanofabrication, with the capability to deposit both biomolecules and electrode materials. This review highlights this new tool for fabricating nanoscale bioelectronic devices, and for enabling heretofore unrealised experiments in the response of living cells to tailored nano-environments. We firstly introduce bioelectronics, followed by a survey of different lithography methods and their use to achieve paradigmic bioelectronic architectures. We then focus on dip-pen nanolithography, highlighting the range of bioelectronic materials and biomolecules which can be deposited using the technique, as well as its demonstrated use as a lithography tool in nano-biology. We discuss the progress made towards upscaling the DPN technology towards larger areas, in particular via the polymer pen approach.

Introduction

Medical bioelectronic (or 'bionic') devices restore human function by interfacing electrical technology with the body.[1] Proven treatments include the Cochlear Implant (or "bionic ear") which has restored useful hearing to hundreds of thousands of patients with profound deafness,[2] and the deep brain stimulator, which has provided significant relief to sufferers of Parkinson's disease and chronic pain.[3] Many other devices are currently in development, such as implants to restore vision,[4] to restore limb movement[5] and as a means to control epileptic seizures.[6] In recent years, the use of electrical stimuli to encourage and direct regrowth of damaged tissue has also been explored.[7–10] The functional interface between any bionic device and the body is at the electrode, which locally stimulates electroactive tissue.[11]

Current bionic devices use electrodes with geometrical areas of ~mm^2, where each electrode addresses thousands of cells. The performance of many bionic devices, particularly those designed to restore sensory function, could be greatly improved by fabricating arrays of many smaller electrodes, with each electrode targeting fewer cells.[12] **Figure 1** compares a conventional cochlear implant with macro-scale platinum ring electrodes with a high density array implant as fabricated by Allitt et al., 2011. The high density array resulted in less activity at nonspecific frequency regions in rat brains and produced significantly lower thresholds and larger dynamic ranges than the platinum ring electrode array.[12]

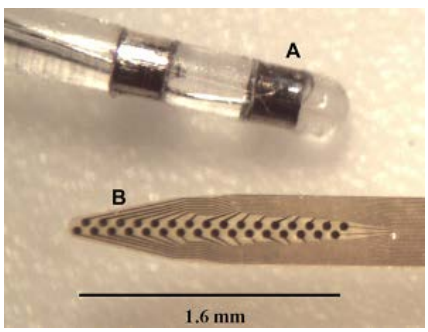

Figure 1: (A) The electrode array of a conventional cochlear implant consists of a platinum ring electrodes around a polydimethylsiloxane (PDMS) shank. (The figure shows a model fabricated for implantation into a rat.) (B) High density electrode array (HDA) of 32 iridium activated stimulation sites along a polyimide shank. The HDA resulted in less activity at nonspecific frequency regions of the inferior colliculus than the platinum ring array. The HDA also produced significantly lower thresholds and larger dynamic ranges.[12] [Reprinted from *Hearing Research*, 287/1-2, Allitt et al., Copyright 2012, with permission from Elsevier.]

Microelectrode arrays of 100 µm diameter have been used to monitor neuronal cell activity *in vitro* for over thirty years.[13] Ideally, however, electrodes would interface with individual cells (cell body <30 µm diameter), or even individual axons (cross-section <500 nm). This goal of electrode miniaturization presents new challenges on several levels. On one hand, the choice of material must be informed by the scaling of relevant properties as the electrode area is decreased. For example, as a gold or platinum electrode is shrunk down, the poor charge injection capacity of noble metals becomes a limiting factor.[14] On the contrary, novel materials may show improved performance at smaller scales; shrinking a conducting polymer electrode can increase the surface/volume ratio resulting in a relative increase in redox switching speeds.[15] On the biological side, the interaction of cells with micron- and nano-scale features must be understood. Research over the past decade has confirmed that living cells feel and respond to topographical and chemical patterns with dimensions on the order of tens of nanometres.[16–18] An inability to create structures of novel materials at nanometre lengthscales will ultimately hamper development in both materials and understanding of the cell-material interface. The design of bionic devices with structure on the nano-scale constitutes the merging of bionics with nanotechnology, heralding the advent of 'nanobionics'.[19,20]
Others have highlighted several emerging technologies for fabricating model substrates with predesigned, nanodimensional architectures.[21] This review highlights AFM printing, also known as dip-pen nanolithography (DPN), as a unique enabling tool for nano-scale bioelectronics and biology. Though we focus on conducting materials, we also touch on the capability of the technique to create nanoscale structures from biomaterials and hydrogels, and incorporating tailored patterning of functional groups, proteins, and cell-adhesion molecules. The technique has enabled the design of new experiments to answer fundamental questions in nanoscience and fundamental cell biology which were previously unanswerable.

Nanofabrication for bioelectronics

We begin with an introduction to nanofabrication, and a brief perspective on how traditional nanofabrication techniques have been used to create bioelectronic architectures.
Nanofabrication has been defined as the process of making functional structures with arbitrary patterns having minimum feature size less than 100 nm in at least two spatial dimensions.[22] Recent reviews of the latest developments in nanofabrication can be found in the literature.[22–24]

The fabrication of nanostructured bioelectronic devices poses a number of unique challenges. Recent work has highlighted how an artificial biomaterial must be as soft as the tissue with which it is integrated.[25] A nanostructure which emulates the extra-cellular matrix is also desirable.[26] Additionally, the device may be loaded with drugs for the controlled release of anti-inflammatories or growth factors.[27,28] Future devices are envisaged to be laced with chemo-attractants to encourage interface with specific cell types. Fabrication of such devices will require structure on a hierarchy of scales from macro-, to micro- to nano-. It is unlikely that any one fabrication strategy will meet all of these requirements. We focus here on the fabrication of nano-scale elements only.

Photolithography

The micro-processor has been described as the most complex device ever manufactured.[29] The drive to keep pace with Moore's law of periodically doubling transistor density has fuelled investment in ever more highly sophisticated photolithography systems over six decades.[30] The resolution of the most advanced photolithography facilities is currently less than 20 nm, at least for inorganic semiconductors and metals.[31] The main limitation of high-end photolithography is its prohibitive expense for most applications. The capabilities available to most bioelectronics research laboratories are relatively unsophisticated and operate on the micro-scale.
The basic procedure of photolithography involves coating a substrate with a thin layer of photoresist and exposing it to UV light through a patterned mask. The UV light effects a chemical change in the photoresist which changes its solubility in a developer solution. Selective removal of the pattern exposes the substrate to further processing steps.
Photolithography has been used to fabricate high-resolution semiconductor devices for investigating the electrode interface at a single cell level. The Fromherz group at the Max Planck Institute for Biochemistry in Munich have been pioneers in this field.[32] For example, **Figure 2**A shows a hippocampal neuron cell cultured on an electrolyte-oxide-silicon (EOS) field-effect transistor, and Figure 2B shows a schematic cross section of the neuron on transistor with blow-up of the contact area.[33] Signal transduction occurs via current in the cell membrane (flowing during an action potential) creating an extracellular voltage in the cleft and thus modulating the source–drain current. Photolithography has also been used to fabricate arrays of individually addressable 2 µm diameter electrodes for the localized stimulation of neurons with sub-cellular resolution. Figure 2C shows a scanning electron micrograph of a primary hippocampal neuron (3DIV) on top of such a micro-electrode array chip.[34]

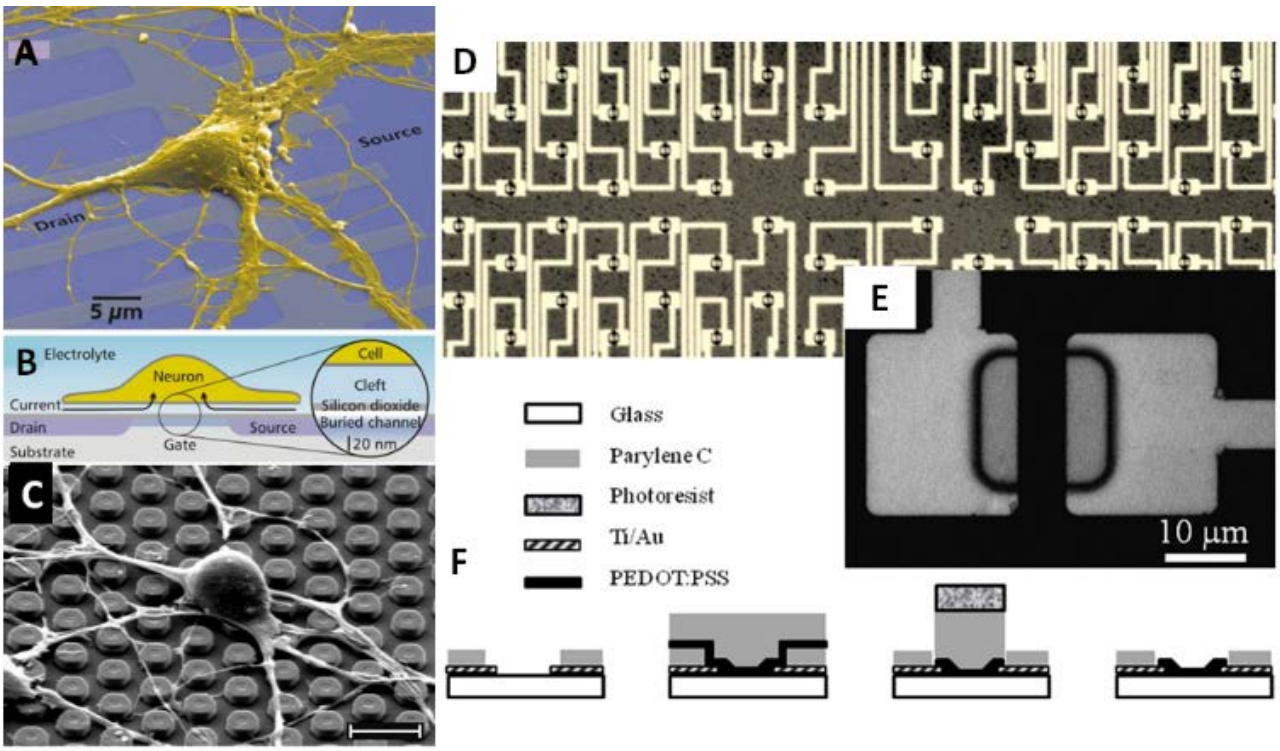

Figure 2: High density electrode arrays fabricated by photolithography. (A) Scanning electron micrograph (colorised) of a hippocampal neuron cultured on an electrolyte-oxide-silicon (EOS) field-effect transistor and (B) schematic cross section of a neuron on a buried-channel field-effect transistor with blow-up of the contact area. [Reprinted from reference[33] with permission from John Wiley and Sons.] (C) Scanning electron micrograph of a primary hippocampal neuron (3DIV) on top of a micro-electrode array chip (TiN coated tungsten electrodes in SiO_2). Scale bar 5 μm. [Reprinted from reference[34] with permission from Elsevier.] (D) A high density array of 64 organic electrochemical transistors (OECTs). The transistors were composed of a 6 μm long poly(3,4-ethylenedioxythiophene):poly(styrene sulfonate) channel contacted by gold electrodes.[35] (E) The inset shows a magnified view of an individual OECT in the array, and (F) shows a schematic of the photolithography process. [(D-F) reprinted with permission from reference[35] AIP Publishing LLC.]

Although highly successful for fabricating devices from metals and crystalline semiconductors, photolithography processes are usually tailored to specific materials and harsh developer solutions may be incompatible with the non-conventional materials (such as soft, organic conductors) ear-marked for bionic applications.[20] Novel processes are being developed to extend photolithography to organic materials. For example, the Malliaras group at the Ecole des Mines de Saint Etienne (formerly Cornell University) has shown how organic electronic devices can be fabricated through a parylene lift-off approach.[36] The group have fabricated a range of devices to interface with living cells, in particular organic electrochemical transistors capable of detecting neurotransmitter release from single neurons[37] and flexible, highly conformal devices for *in vivo* recording.[38] Figure 2D shows a high density array of 64 organic electrochemical transistors (OECTs) fabricated by the Malliaras group. The transistors were composed of a 6 μm long poly(3,4-ethylenedioxythiophene):poly(styrene sulfonate) channel contacted by gold electrodes.[35] Though fabrication of organic electronic devices in this manner is very promising, at present the feature size is limited by the lift-off process at >1 μm.[36]

The technique of deep reactive ion etching (DRIE), is related to photolithography as it involves building a structure using a succession of masking steps. The patterns are defined by excavating trenches using a plasma etch however, rather than light-activated chemistry. The trenches are then filled (e.g. electrochemically) to form electrodes. This technique has been explored by the Wise group at the University of Michigan to fabricate high density cochlear electrodes and as well as cortical electrode arrays capable of single-unit recording.[39,40]

Scanning beam lithography

Scanning beam lithography (SBL) is a direct-write technique where a spot of a tightly focused beam is used to generate a pattern by either the selective removal of material or the selective deposition of a species. SBL is very slow (requiring up to 24 hours per cm^2 for 20 nm scale features)[22] but its high resolution and pattern fidelity make it a critical technology for the fabrication of masks for photolithography. SBL has also been used in niche research applications in bioelectronics. Figure 3A shows an array of nanowire transistors fabricated by the Lieber group at Harvard for their pioneering work in interfacing with neuron cells. The group succeeded in interfacing a single axon with a linear array of 50 SBL fabricated nanowire devices and thus monitor the propagation of an action potential [41]

Micro- and nano-contact printing

The contact printing technique uses a patterned elastomeric stamp (typically PDMS) to transfer molecules to a substrate, typically via the formation of covalent bonds (e.g. self-assembled alkanethiols on gold).[42,43] Resolution is determined by the feature size of the stamp. Although typically used to generate micron-scale features, sub 100 nm resolution has been demonstrated.[44] Limitations to feature size arise from the fidelity of the molding process used to create the stamp, the properties of the stamp material (e.g. ability to retain nanoscale

features) and distortion of the stamp while in contact with the surface.[22]

The major advantage of contact printing is its low cost.[23] The technique has been widely adopted by the biomedical research community for applications such as; patterning ECM proteins for controlling cellular adhesion,[45] fabricating model substrates to study cellular biomechanics[46] and for creating bio-molecular gradients.[47] Figure 3B shows a biomolecule array generated by µCP for an in vitro study of cellular spreading as a function of ECM geometry. B16 (murine myeloma) cells were cultured on substrata patterned with different geometrical arrangements of the cell adhesion protein fibronectin. The degree of spreading was found to be dependent on spacing of the fibronectin features.[48]

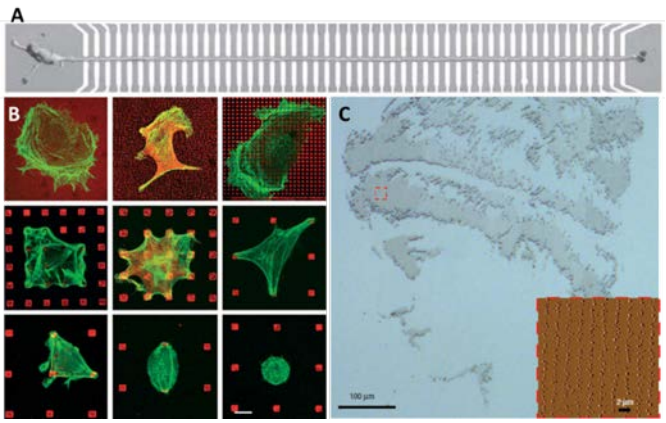

Figure 3: Fabrication by scanning beam lithography (SBL), micro-contact printing (µCP) and electrohydrodynamic jet (e-jet) printing. (A) SBL was used to fabricate a linear array of fifty nanowire (NW) transistors. Axon growth was direct along the NW junctions by patterning poly-L-lysine. The array of transistors used to follow the propagation of an action potential along the axon.[From reference[41], reprinted with permission from AAAS.] (B) The images show B16 (murine myeloma) cells cultured on fibronectin substrata as patterned by µCP and labelled for fibronectin (red) and actin (green). The degree of spreading was found to be dependent on spacing of the fibronectin features. [Reprinted from the Journal of Cell Science[48] with permission from the Company of Biologists Ltd.] (C) High resolution liquid deposition by e-jet printing. Optical micrograph of a portrait of the ancient scholar, Hypatia, printed using a polyurethane ink and a 500-nm-internal-diameter nozzle. The inset shows an AFM image of the printed dots.[Reprinted by permission from Macmillan Publishers Ltd, reference[49] copyright 2007.]

Jet printing

Although ink-jet printing (IJP) was initially developed for the publishing industry, it has been adopted as an important and versatile technique for direct-write deposition of many functional materials.[50] One unique prospect of IJP is incorporation of living cells within the ink, leading to the possibility of 'bio-fabricating' structures composed of both material and living components.[51,52] IJP is ostensibly a micro-scale fabrication technique, with a lower limit of droplet size in the pico-litre range, corresponding to resolution on the order of ~10 um.

A technique related to IJP, known as electrohydrodynamic jet printing (e-JP) has been recently devised which can jet femto-litre and even atto-litre volumes, corresponding to droplets with diameter on the ~200 nm scale.[49,53] Resolution is dependent on liquid properties, substrate wettability and the diameter of the jet nozzle. e-JP is promising, however it is limited in that a conductive substrate must be used. Figure 3C shows a pattern e-jet printed using a polyurethane ink and a 500-nm-internal-diameter nozzle. Individual dots have a diameter of ~490 nm.[49]

Scanning Probe Lithography

Scanning probe microscopes (SPMs) are a family of tools which use a physical probe, usually a tip with nanoscale sharpness, to scan back and forth and make images of nanoscale surfaces. Though primarily tools for characterisation, SPMs been used to fabricate many paradigmic nanostructures not achievable by other means, from patterns of individual positioning of xenon atoms,[54] to the smallest field effect transistor.[55]

The atomic force microscope (AFM) in particular has borne a rich suite of fabrication tools utilising the precise delivery of mechanical forces, thermal energy, electrical bias or materials deposition. [56–60]. For a recent review of advanced scanning probe lithography (SPL) techniques, see this reference.[61]

The simplest form of AFM lithography is to use the AFM tip literally as a nanoscale 'pick' or 'shovel' to scratch or cut into a substrate. The technique has been used to 'nanomachine' gold nano-wires,[56] and to create electronic devices from semiconductors such as gallium arsinide.[57] Thermomechanical AFM lithography is a variant where the probes are heated to aid indentation of soft polymers.[62] This technique is exemplified by IBM's Millipede device, which was equipped with an array of 1064 individually addressable, locally heated probes, allowing for read-write-rewrite capabilities.[63]

In AFM nanografting, nanoscale regions of a self-assembled organic layer are shaved away by the AFM tip and a second molecule adsorbs to fill in the pattern with resolution approaching the sharpness of the tip (~10 nm), see Figure 4A.[64] Besides secondary SAM molecules, both proteins[65] and nanoparticles[66] have been nanografted.

In local oxidation nanolithography (LON) an electric bias is applied between the tip and substrate, inducing ionic dissociation of the water meniscus between tip and sample, and forcing a downward acceleration of negatively charged species (OH^-, O^-) towards the surface. In the case of a silicon substrate, the OH^- anions combine with holes at the surface resulting in the localised growth of SiO^2. The technique has been used to push the fabrication limits of devices such as metal-oxide-semiconductors via nanoscale definition of the local oxide growth.[58,59] Figure 4B shows, at left, a generic schematic of the LON technique and, at right, a nanoscale oxide structure fabricated by LON for fundamental quantum mechanical experiments in ring geometries.[67] Some efforts at upscaling the technique have been made, for example the Quate group at Stanford have used arrays of up to 50 cantilevers to effect centimetre scale lithography.[68]

The AFM lithography techniques described above generate a pattern by delivering energy to selectively remove or modify a pre-existing substrate. The innovation to use an AFM tip to deliver *material* opened up totally new possibilities for AFM lithography.[69] In a concept known as "Nano-fountain probe" or "liquid nanodispensing", material is delivered a nanochannel through the AFM tip.[70–72] This approach has demonstrated versatility through the printing of gold colloids,[73] DNA[74], and proteins.[75] The design has allowed for some unique applications, for example, the injection of single cells with nanoparticles (Figure 6C).[60]

An impressive innovation in recent years has been the advent of lithography using modified scanning ion conductance microscopes. Conducting polymer nanostructures can be synthesised in situ at the apex of a nanopipette.[76] In another

approach, freestanding metal electrodes have been fabricated via the meniscus-confined electrodeposition of copper or platinum (Figure 4D).[77]

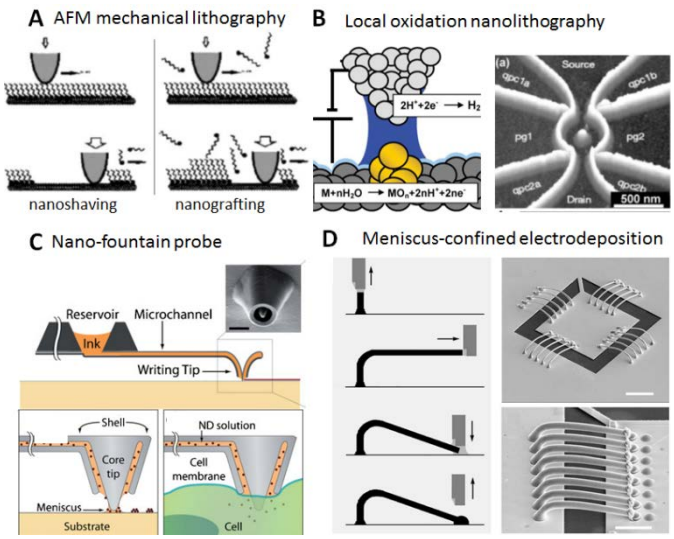

Figure 4: Selected scanning probe lithography strategies: (A) AFM nanoshaving involves the selective removal of an organic SAM from a metal or oxide surface using mechanical force applied by an AFM tip. When nanoshaving is performed in a solution of secondary SAM molecules, the shaved regions are 'nanografted' with the secondary SAM. [Adapted with permission from Liu et al, Accounts of Chemical Research 33, 457–466. Copyright (2000) American Chemical Society.][78] (B) [Left] In local oxidation nanolithography (LON), the applied field induces ionic dissociation of the water meniscus between tip and sample and the oxidative OH- anions migrate to the substrate and react with it to form localised oxide structures. [Schematic reproduced from reference [79] with permission from The Royal Society of Chemistry.] [Right] LON has been used to create novel nanoelectronic architectures by patterning local oxide on semiconductors [Reprinted by permission from Macmillan Publishers Ltd: Nature 413, 822–5, copyright (2001).][67] (C) The nanofountain probe (NFP) incorporates microfluidic channels inside the cantilever to deliver liquid or molecular ink from a reservoir to the writing tip. The design allows for not only deposition of ink on substrates, but also the injection of ink (in this case a nanoparticle solution) into living cells. [Copyright © 2009 Wiley-VCH Verlag GmbH & Co. KGaA, Weinheim. Reproduced with permission,][60] (D) The nanopippete of a scanning ion conductance microscope can be used to fabricate free-standing metal electrodes via electrodeposition confined to the contact meniscus formed between the pipette and the substrate. [From reference[77], reprinted with permission from AAAS.]

Dip-pen nanolithography

Dip-pen nanolithography (DPN) is one further candidate technology for fabricating novel substrates tailored at the nano-metre scale. DPN is a constructive lithography technique which uses an atomic force microscope (AFM) tip to deposit molecules or materials in a direct-write fashion.[80] Key to the technique is the fact the AFM cantilever is 'dipped' into the ink and thus coated—an approach that extends versatility by avoiding the clogging of nanofluidic channels. It is of particular interest to the bioelectronics community as many of the essential ingredients of prospective bioelectronic devices can be printed: including metals,[81–85] insulators[86] and conducting polymers.[87–89] DPN also enables the nanoscale patterning of biomolecule cues through the deposition of DNA and proteins.[90,91] The capability to 'multiplex' many different biomolecules within a subcellular area allows for the creation of complex substrates tailored with biomolecules on the nanometre scale, with huge implications for both fundamental and applied cell biology.[92] The non-destructive nature of DPN means it is compatible with many substrates including soft, flexible polymers[93] and even biological tissue.[94] Although AFM based lithography has traditionally been regarded as a serial, and therefore slow fabrication technique, great strides have been made in parallelization of DPN; first to "massively parallel" 55000 cantilever arrays,[95] and more recently using polymer pen lithography (PPL) arrays capable of simultaneously printing up to 11 million patterns over cm^2 areas.[96] DPN is already finding use as a tool for fabricating novel nano-patterned cell-growth platforms for fundamental cell-biology studies.[97–101]

Particularly unique is the ability of DPN to manipulate minute quantities of liquids.[85,91,93,102] Liquid inks are interesting in the biomedical field for their ability to operate as 'universal' carrier matrices for biomolecules.[91] The patterning of hydrogels is fascinating as it may also provide a novel means to tailor a heterogeneous soft material interface at the nano-scale.[102] Liquid deposition patterning is usually not substrate specific and so is versatile enough for printing on a variety of hard and soft substrates.[93] The development of liquid ink DPN may also by accelerated by the adaption of many hundreds of strategies already developed for other liquid printing techniques, such as ink jet printing.[50]

In the paradigmic DPN system, alkanethiol molecules are adsorbed onto an AFM tip. When the tip is brought into contact with a gold surface, a water meniscus is formed via capillary condensation and the alkanethiol molecules diffuse through the meniscus and bond to the surface.[80] Most DPN strategies prescribe to this mechanism of diffusive molecular transport. Viscous liquid inks are deposited via a different mechanism, critically dependent on the growth of the ink meniscus itself,[103] and can be subject to hydrodynamic effects which can impact on the uniformity of deposition.[104]

Bioelectronic Materials Deposited by AFM Nanoprinting

A range of methodologies have been developed over the past decade to print metal features via DPN (see Table 4-1 for a summary). Many of the DPN approaches concern the patterning of metal nanoparticles, in particular functionalised Au nanoparticles, for sensing or bio-recognition applications.[66,73,105–107] Although interesting for the varied approaches used to effect ink-transfer (e.g. ink-substrate hyrophobicity, nanografting etc), the presence of insulating capping agents precludes many of these strategies from generating conductive lines. One nanoparticle based methodology did target the deposition of conductive traces by including silver nanoparticles in a glycerol thickened ink formulation.[84,85] A relatively high conductivity was achieved ($3x10^4$ S cm^{-1}) using an annealing temperature of 150 °C.

The surface activated *in-situ* redox approach utilises opportune surface chemistry to effect reduction of a metal precursor ink upon deposition.[108,109] *In-situ* reduction has been achieved for Au and Pd on bare Si (from which the oxide layer was removed

by hydrogen fluoride) and Ge substrates. Although extending this approach to flexible materials may be possible, it would require pre-functionalising the substrate with a suitable electron donating ligand.

Table 4-1: Selected DPN metal printing studies.

Met	Sub	Method	Res (nm)	
			Dot	Line
		Direct deposition of NPs		
Au	SiOx	Au NPs; hydrophobic modified[105]	50	-
Au	Au	Nanografting on thiolated Au[66]	-	150
Au	mica	Functionalised NPs, DPN in solution[106]	-	40
Au	-NH_2/ SiOx	Nanofountain pen, functionalised NPs[73]	200	-
Ag	SiOx, Kapton	Ag NP ink, 150 °C cure[84,85]	-	500
		Thermal DPN		
In	SiOx	Heated tip, 250-500 °C[82]	-	50
		Surface activated in situ redox		
Au	Si (HF treat)	$HAuCl_4$ in situ redox on elemental Si[108]	<100	<100
Au,Pd	Ge	In situ redox on Ge[109]	-	30
		Electrochemical DPN		
Pt, Au, Ag	SiOx	H_2PtCl_6 reduction with 4V bias applied to tip[81]	-	30
Au	OTS/ SiOx	Electrograft Au NPs on OTS SAM[110]	-	50
		Chemically directed assembly (CDA) of NPs		
Au	Au	Au NPs on amine terminated patterns[111]	-	<100
		Seeded growth		
Au	Ag/ SiOx	Thiol pattern and etch Ag, reduce $HAuCl_4$ on Ag[112]	1000	-
Ag	Au	Electroplate Ag on thiol patterned Au[113]	190	170
Au	SiOx	+12V bias, Au NPs, seed growth of $HAuCl_4$[114]	-	250
Au, Ag	SiOx	Print NP tagged enzyme $HAuCl_4$ growth solution[115]	-	500
		Wet etching a metal coating		
Au	SiOx	DPN print ODT resist and wet etch[83]	~50	~50
Au	SiOx	Polymer pen MHA resist and wet etch[96]	~50	~50
		Electroless deposition		
Au, Pt	HMDS / SiOx	Print metal precursor loaded block-copolymer micelles, O_2 or Ar plasma treat[116]	5	-
Au	SiOx, Al_2O_3, polyimide	Thermal DPN deposition of $HAuCl_4$, annealing at 270°C. [117]	50	55

Reduction of a metal precursor within the contact water meniscus by applying a bias between pen and substrate (i.e. electrochemical DPN) has been used to nanopattern both Pt[81] and Au[110] at line resolution down to 30 nm. This approach, however, necessitates a conducting or semi-conducting substrate, limiting its utility on flexible polymeric materials. The seeded growth approach uses the metal pattern as a seed site for the reduction of a metal precursor in a post-treatment growth step.[112–115] The idea is interesting as a augmentation to other printing methods (e.g. to improve pattern continuity),[114] but is not a printing methodology in itself.

Nanopatterning a thiol resist against the wet-etch of a metal coating is the most popular method in the literature for generating conductive metal patterns by DPN.[96,113,118] This method can achieve micro- or nanoscale resolution (<50 nm) and upscalability to millions of features over cm^2 areas (via polymer pen lithography).[96] The method also does not compromise electrical properties as the pattern will retain the conductivity of the thermally evaporated metal thin film. Most of the work thus far has focused on gold, although both Ag and Pd patterning have been demonstrated.[119] Extending this approach to Pt presents significant challenges, however. The only known etchant for Pt metal is the highly corrosive aqua regia (a mixture of concentrated nitric and hydrochloric acids in a 1:3 ratio). The effectiveness of a thiol SAM to protect against an aqua regia etch is yet to be demonstrated.

Recently, the Mirkin group adapted 'block copolymer lithography' for both DPN and PPL techniques.[116] Their ink was based on block-copolymer micelles loaded with metal ions ($AuCl_4^-$ or $HPtCl_6^-$). After printing of the micellar ink, an oxygen plasma treatment effected reduction of the metal ions by a hydrocarbon oxidation mechanism. Although a landmark study, as the features generated (~4.8 nm) were smaller than the radius of the pen used to print them (~15 nm), this approach was limited to patterning of single dots, and not continuous lines. The micellar vehicles define the minimum proximal distance between features at about 500 nm.

A final approach is the electroless deposition of metal precursors is to DPN print a metal precursor salt and subsequently reduce the salt via heat treatment *in situ.* THis strategy has been used to fabricate gold patterns using a locally heated DPN tip.[117] Both dots and lines were deposited on various substrates, however a reduction temperature of 270°C was required, which may not be amenable to polymeric substrates. Our group have since extended the electroless deposition approach to print nanoscale platinum features on sensitive substrates by using a mild plasma treatment to effect reduction of the printed precursor.[120]

One of the first application-orientated DPN studies exploited patterned alkanethiols as etch resists to form gold and silicon nanostructures, highlighting the potential of DPN in the fabrication of nanoelectronics with <20 nm resolution and arbitrary pattern design.[83] This methodology has been successfully upscaled to polymer pen lithography.[96] In working devices, nano-scale electrodes are often addressed by macro-scale electrodes made using conventional photolithography. Some methods for achieving registry between DPN and micro-fabricated structures have been described.[121] One highlight has been the definition of electrical contacts to single graphene flakes under ambient conditions.[122] Another potential

application which has been cited is the inspection and repair of defects in prefabricated photomasks[123] and in integrated circuits.[85]

DPN of conducting polymers has been achieved by several methods including; electrostatically driven transport,[89] electrochemical DPN,[87] in situ polymerization[88] and direct writing of soluble CP.[124] The approaches are outlined in Table 3-1. Such approaches have been used to create organic electronic devices exhibting fast switching speeds.[124] The capability of liquid ink deposition to fabricate conducting polymer electrodes on a variety of flexible substrates shows promise for pushing the limits of organic bioelectronics devices. [93,125,126]

Table 3-2: Selected DPN conducting polymer printing studies.

Poly-mer	*Sub*	*Method*	*Res (nm)*	
			Dot	*Line*
Ppy, SPAN	Si, Au	Electrostatic driven transport[127]	130	290
PEDOT	SiO_2	Electrochemical DPN[87]	-	50
Ppy	SiO_2	In situ polymerization of monomer ink[88]	500	200
PEDOT: PSS	SiO_2	Meniscus transport of soluble CP[124]	-	300
PEDOT: PSS	Si/SiOx, SiO2, PDMS, PET	Liquid ink deposition[93]	800	-
PEDOT: TOS	Si/SiOx, SiO2, PDMS,	Deposition of oxidant and vapour phase polymerisation[125]	1000	~250
PEDOT: PSS	Si/SiOx, SiO2,	Liquid ink deposition[126]	100	-

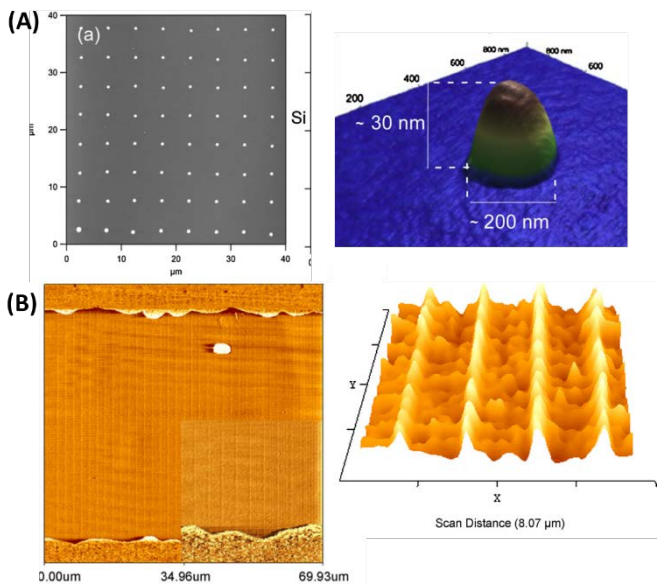

Figure 5: DPN printed conducting polymers approaching nanoscale resolution. (A) PEDOT:PSS features fabricated via DPN liquid ink deposition. On left is an AFM topographical image of an array of uniform PEDOT:PSS dots. On right is a 3D rendered AFM topography image of a single PEDOT:PSS feature. [Reproduced from Wagner et al[126], Copyright Elsevier 2012 (permissions pending)] (B) PEDOT PSS lines (300 nm width) bridging two metal electrodes and forming an NO gas sensor. On left is a 2D AFM image of the patterned lines. On right is a 3D rendered AFM topography image of the same line features. [Reprinted from reference[124] with permission from Elsevier.]

Nano-biology Applications

As DPN can operate in an ambient environment, and with little or no post-treatment, fragile biological structures such as DNA[128] and proteins[129] could also be printed at nanoscale resolution while retaining their native structure. A biomolecule carrier ink has been developed for versatile printing of proteins or oligonucleotides with consistent deposition rates.[91] The possibility of patterning hydrogels and lipids at nanoscale dimensions also has numerous potential applications in the patterning of a soft localised cellular nanoenvironment.[92] DPN has also been used to pattern virus particles,[130] and even a bacterial 'ink' has been developed.[131] The dozens of methods to DPN print biomolecules, by both direct and indirect methods, were reviewed in 2011.[132]

BIOMOLECULE NANOARRAYS One of the applications for which DPN seems most immediately suited are in the generation of biomolecule nanoarrays for high through-put screening assays in proteomics, genomics and drug development.[69] The powerful potential of nanoarrays in biomedicine is illustrated by an example outlined by Mirkin:[123] A DNA array capable of identifying any known sequence would require 4 x 10^{17} features and so a micro-array with 50 µm features would be approximately the size of a tennis court. A nanoarray with 50 nm features would be only ~1 cm^2, making such a chip practical in real world applications.

The first proof of concept of a DPN printed nanoarray used for diagnostic purposes was demonstrated by the Mirkin group in 2004 (Figure 10A).[133] Nanoarrays of antibodies against the HIV-1 p24 antigen (anti-p24) were created by electrostatic binding to MHA nanopatterns. HIV-1 p24 antigen in plasma obtained from HIV-1-infected human patients was hybridized to the antibody array in situ. Detection of the hybridization was via height change (from 6.4 nm to 8.7 nm) as measured by AFM. A gold antibody-functionalized nanoparticle probe was also used for signal enhancement (height change 20 nm). Although a slow and laborious process in this form, the assay achieved a limit of detection of 0.025 pg per ml, exceeding that of conventional enzyme-linked immunosorbent assay (ELISA)-based immunoassays.

Nanoarrays are also important as models for fundamental studies of biomolecular interactions, and have huge potential when coupled with strategies of AFM force measurements. DPN printed nanoarrays of $\alpha_v\beta_3$ integrins or BSA were probed by an AFM tip functionalised with vitronectin.[134] Increased adhesion forces arising from specific interactions could distinguish integrin from BSA. Although still in its infancy, this methodology may lead to a robust model system of studying the interaction force of pairs of biomolecules as a function of solution condition (pH, ionic strength) and conformation, especially with the advent of strategies to generate single-molecule protein arrays.[135]

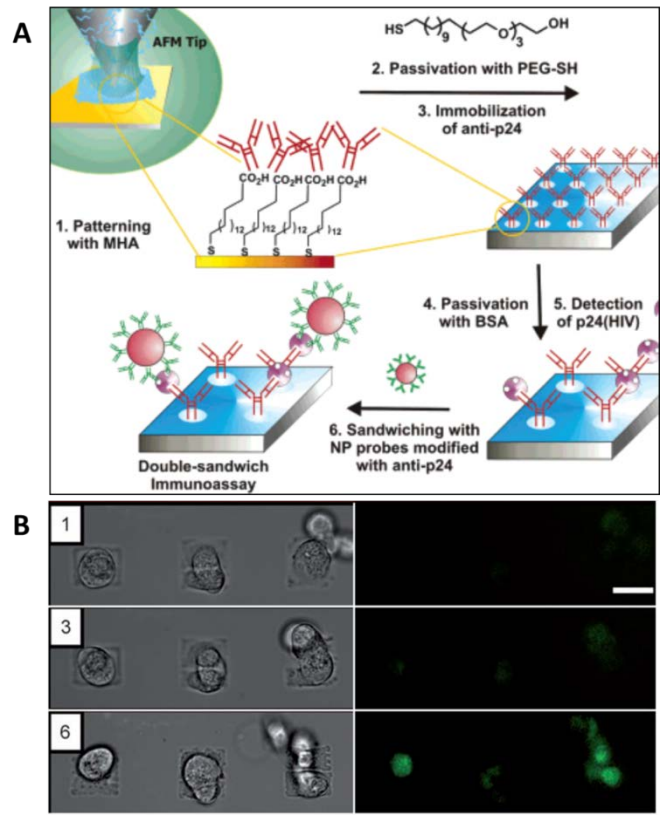

Figure 6: (A) Schematic of the immunoassay format used to detect HIV-1 p24 antigen with anti-p24 antibody nanoarray. The anti-p24 antiobody was immobilized on DPN printed MHA patterns by an electrostatic interaction. Binding of the p24 antigen produced an increase in height of the nanoarray as monitored by AFM. The increased height signal could be amplified using anti-p24 modified gold nanoparticles. [Reprinted from Lee et al., 2004[133], Copyright 2004 American Chemical Society.] ((B) CV1 monkey kidney cells adhering to nanoarrays of rSV5-EGFP virus engineered to express green fluorescent protein (GFP). Infection of the cells by the virus could be monitored by the increased GFP fluorescence over time. [Reprinted with permission from Vega et al.[136] Copyright 2007, John Wiley and Sons]

INFECTIVITY STUDIES The Mirkin group demonstrated the capability of DPN to generate arrays of single virus particles in an active state.[130] The immobilized virus particles were capable of infecting living cells cultured on the arrays.[136] Through the use of green fluorescent protein expressing virus particles, an assay was developed to follow the infectivity process on nanoarrays using fluorescence (Figure 10B). Thus the systematic examination of single-cell infectivity with control of the density and spatial distribution of virus particles has been made possible. The direct write patterning of bacterial cells by DPN was also recently demonstrated, opening the door to similar infectivity studies at the bacterial level as well as possible applications in drug-delivery, biofilms and molecular motors.[131]

NANOPATTERNED MODEL SUBSTRATES FOR FUNDAMENTAL IN VITRO CELL STUDIES An understanding of the processes of adhesion, migration, differentiation in artificial environments is crucial to the development of novel approaches to medicine such as tissue engineering[137] and medical bionics.[20] Model substrates presenting well defined patterns allow for the systematic study of the cell-material interface and have been important for elucidating the spatial and temporal mechanisms of these processes.[138]

Since the 1990s SAMs of alkanethiolates on gold have been a prominent model substrate for fundamental *in vitro* cell studies.[139] Key to their success as a model substrate is the simplicity of their preparation, and the diversity in choice of the presented groups. The ability to pattern these SAMs on the scale of single-cells using micro-contact printing[42] lead to some seminal work in the control of cell-fate by purely geometric means.[140] A generic protocol has become the method of choice for patterning cells:[45] hydrophobic alkanethiols are generated on gold via micro-contact printing and remainder of the substrate is rendered biologically inert by immersion in a solution containing oligo(ethylene glycol) terminated alkanethiol. Hydrophobic alkanethiols permit the adsorption of ECM proteins, and cells only adhere to the patterned areas.

Living cells are sensitive to nanoscale topographic and biomolecular patterns,[16] though the mechanisms by which cells transduce signals from their microenvironment is poorly understood. DPN has allowed for the fabrication of model substrates at the nano-domain, allowing the study of geometric effects at a much finer scale than previously possible, that of individual focal adhesions. The differentiation of human mesenchymal stem-cells (MSC) differentiation was controlled via DPN nanopatterns of various functional groups without the use of differentiation media.[99,100] The size of nanospots was optimized at 70 nm diameter corresponding to the diameter of cellular focal adhesion structures. MSC adhesion and phenotype was dependent on both the terminal functionality (amino, methyl, hydroxyl or carboxyl) and the pitch (140 to 1000 nm) of the nanopatterns. The nanopatterns were shown to influence the formation of focal adhesions through controlling specific integrin clustering, which can then be used to direct cellular response.

Besides nanopatterning of surface chemistry, the capability of DPN to generate biomolecule nanoarrays is enabling the systematic study of biospecific interactions at the nanoscale. Nanoarrays of the cell-adhesion protein retronectin have been used to study the fundamental processes of cellular adhesion.[141] The adhesion of 3T3 mouse fibroblast cells on DPN generated nanoarrays of both linear and cyclic RGD cell adhesion peptides has also been studied.[97] Cells were found to develop eight times more focal adhesions on the cyclic rather than the linear RGD patterns. Cell adhesion was also dependent on spot-size and pitch of the nanoarrays. In a later work, the same group explored this effect further, studying how nanoarray geometry influences cell polarity orientation (Figure 11A).[98] They found that 3T3 cells were polarized on asymmetric arrays, but not on symmetric arrays, of linear RGD peptide. In other work, microspots of fibronectin were also shown to define the morphology of 3T3 fibroblasts (Figure 11B).[142]

A unique advantage of DPN is the capability to create high resolution patterns of multiple ink formulations over a subcellular area. Figure 11C shows fluorescence micrographs of poly(ethylene glycol) dimethacrylateloaded hydrogel

features loaded with four different dyes printed as a multi-ink printing demonstration.[92] Lenhert and Fuchs have printed lipids by DPN with the goal of generating biomimetic membrane patterns as model substrates for cell culture.[143] They demonstrated the multi-plexed printing of lipids with lateral resolution down to 100 nm. By binding functional proteins to lipids containing either a nickel chelating headgroup or a biotinylated headgroup, they could demonstrate the selective adhesion and activation of T-cells. In a related development, the Salaita group used patterns of a cationic polyelectrolyte to impede lipid diffusion and therefore control spatial organization of ligands in membranes and cells.[144]

A particularly exciting outcome of biomolecule nanopatterning is the possibility of localized delivery of drugs to single cells. Figure 11D shows NIH 3T3 fibroblasts cultured on DPN printed microarrays locally delivering Calcein AM (green colored cells), Calcein Red AM (red colored cells) or DMSO (no color cells). Localized intake of the dyes is evidenced by the overlaid fluorescence image.[145] This work highlights the potential for high-throughput, lab-on-a-chip drug screening assays, especially when complemented by advances in multi-inking of large area, massively parallel arrays.[146]

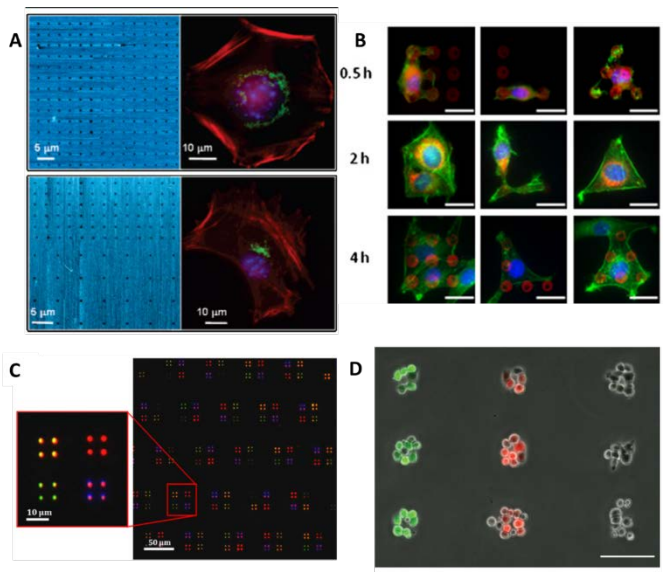

Figure 7: (A) Cellular response to a nanoscale arrangement of binding sites. 3T3 mouse fibroblast cells adhering to symmetric (top) and asymmetric (bottom) nanoarrays of immobilized RGD linear peptide. The diffuse distribution of the Golgi surrounding the nucleus indicates that the cell on the symmetric nanoarray is not polarized, whereas the cell on the asymmetric array is polarized. [Adapted from Hoover et al.[98] Copyright 2008 American Chemical Society:] (B) Controlling cellular morphology with subcellular protein patterns. Fluorescence microscopy of 3T3 fibroblasts attaching to DPN printed fibronectin patterns and spreading over time. At 2 h, cell morphology is defined by the protein patterns. Scale bar = 20 µm. [Adapted with permission from Collins et al.[142] Copyright 2011 Elsevier.] (C) Multi-ink pattern generation over sub-cellular areas. Fluorescence micrographs of poly(ethylene glycol) dimethacrylateloaded hydrogel features loaded with four different dyes—rhodamine/FITC (orange), rhodamine (red), Alexa347 (blue), and, FITC (green) [Reprinted from Stiles et al.[92] copyright 2010 MacMillan Publishers Ltd] (D) Targeted drug delivery. NIH 3T3 fibroblasts cultured on DPN printed microarrays locally delivering Calcein AM (green colored cells), Calcein Red AM (red colored cells) or DMSO (no color cells). [Adapted from Collins et al 2012,[145] with permission from the Royal Society of Chemistry.]

Upscaling DPN

Early DPN experiments were considered very low throughput as they used only single pen or limited linear pen-arrays. The limitation of upscalability has been addressed by successive examples of increased parallelization;[123] the 32 cantilever linear pen array was introduced in 2002,[147] and the 55,000 cantilever 2D 'massively parallel' pen array in 2006 (though whole wafers of 1.3 million pens were also fabricated as proof of concept).[95] Although they were commercialised, the pen arrays were fragile, expensive to fabricate and required a labour intensive levelling process.[148]

Invention of polymer pen lithography

The efforts toward parallelization culminated in 2008 with the invention of polymer pen lithography (PPL).[96] PPL presented an elegant 'cantilever-free' solution to the problem of increasing pen density array using a PDMS stamp of thousands of nano-sharp pyramidal tips. The PDMS stamp could fabricated using a Si mould, greatly simplifying the pen fabrication process, and reducing the material cost per 'stamp' to just $1. PPL represented the convergence of large area but pattern specific soft-lithography with small area, direct write DPN.[149]

In the past five years, significant advances have been made in improving the practicality of PPL. A clever solution to the multi-plexed inking of PPL stamps was found in using the silicon master (used to fabricate the stamp) as the ink-wells. Ink-jet printing was used to fill different 'ink wells' with different proteins.[146] A method of levelling the stamp with the potential of automation was developed which uses the force applied by a non-levelled stamp on the substrate as the basis for a feedback loop.[150]

An additional parameter to be considered with PPL is that, in contrast with DPN, feature size is force dependent.[96] This can be advantageous as feature size can be controlled without relying on environmentally sensitive diffusion processes.[151] However, the deformation of the PDMS tips does place a resolution threshold on the technique. The contamination of printed features with molecules of PDMS (a problem in soft-lithography) is also left open. A recent development, dubbed 'hard-tip soft-spring' lithography, addresses these issues by using a PDMS stamp capped in silicon oxide.[152]

PPL has been used for the large area patterning of the cell adhesion protein fibronectin as a means to rapidly screen the influence of fibronectin feature size on the adhesion and differentiation of human mesenchymal stem cells (MSCs).[101] MSCs cultured on optimised nanopatterns of fibronectin differentiated towards osteogenic fates, even without media containing osteogenic-inducing chemical cues.

An intriguing spin-off technology from PPL, dubbed 'beam-pen lithography' (BPL), has enabled a maskless, direct-write parallelization of photolithography.[153] In BPL, 400 nm light is passed through nanoscopic apertures in the polymer pen tips, to

generate thousands of sub-wavelength (100 nm) spots. Piezo-electric manipulation of the polymer pen allows for generation of arbitrary photolithographic patterns.

The progress in up-scaling the DPN technology over the past decade has been impressive. For example the printing time to deposit 1 billion features has decreased 5 orders of magnitude over three generations of DPN systems.[149]

'Active' probe arrays

Besides up-scalability, some limitations to DPN do remain. In particular, the major advances in parallelisation have utilized passive pen arrays. Although millions of tips over multi cm^2 areas can engage in printing simultaneously, a passive pen array can only generate duplicates of a single design. 'Active' parallel probe arrays consisting of individually addressable cantilevers have been demonstrated using both thermally activated and electrostatically activated probes.[154,155] Such inventions could lead to a vast increase in the possible pattern complexity would be achieved, particularly if combined with multi-plexed printing. No active probe system for a 2D DPN probe array has been reported. However, IBM Zurich did demonstrate the actuation of individual cantilevers in a massively parallel arrangement during the development of their 'Millipede' memory storage device.[63]

Summary and outlook

In the past decade DPN has become increasingly recognized as a powerful tool for creating designer substrates using nano-scale, molecular building blocks. The huge versatility afforded by the availability of hundreds of demonstrated ink-substrate systems has piqued the interest of researchers from a wide range of disciplines. The ability of DPN to deposit metal and organic conductors at nanoscales, and on a range of substrates, could prove important for bridging the world of bioelectronics with nanoscience.

The impact of DPN on the biological sciences has grown. In recent years, several breakthroughs in understanding stem cell differentiation have been made possible using DPN nanoarrays. However, much of DPN's potential is as yet untapped. In particular, the recent advances demonstrating multi-ink protein patterning over large areas have yet to be utilized to address long standing questions in fundamental cell biology, such as the complexities of how cell phenotype is influenced by multiple signaling proteins arrayed on a surface.

The invention of polymer pen lithography has enabled the high resolution printing of DPN to be up-scaled to millions of simultaneous patterns in a cost-effective manner. Multi-plexed inking strategies have also been developed, but pattern complexity still remains restricted by limitations imposed by the passive probe design. The greatest potential of DPN/PPL technology will be only unlocked when multi-inking strategies are married with individually addressable, massively parallel active pen arrays. A good understanding of the parameters affecting molecular ink transport has been compiled. However, much further work is required to achieve a similar level of understanding for liquid ink deposition.

There are as yet no examples of DPN being used to create standalone bioelectronic devices, yet it promises to have a significant impact when use in conjuction with more traditional techniques, as surveyed in the opening section of this review. The capability of DPN to deposit organic conductors and molecular coatings could be used, for example, to achieve localised augmentation and funcntionalisation of prefabricated electronics at nanoscales.

Perhaps the most unique capability of DPN is its versatility in being able to deposit both biomolecules and conductors at room temperature and in an ambient environment. This opens the door to the possibility, as yet untapped, to fabricate integrated systems incorporating both biomolecule and conducting components. Conducting polymers containing biomolecules, and even red blood cells, as part of their matrix have already been synthesised.[156,157] Using available technology, one can envision the use of DPN to create conducting polymer electrodes which could be nanopatterned (or even locally doped) with multiple biomolecules, or biomolecular gradients, at nano-scales. Patterned chemoattractants, for example, could be used to control the formation of 2D neuronal networks or neuromuscular junctions, or to study the fundamental processes of axon guidance.

DPN, like other SPM based lithography tools, is in its element in a research setting. The technology provides a means to fabricate novel structures. We have highlighted capabilities such as the arbitrary patterning of individual 5 nm nanoparticles,[116] or individual proteins,[135] and the patterning of multiple different proteins within subcellular areas[142] which are not achievable by other means. These tailored nanoenvironments, and others, will continue to justify DPN and PPL as enabling tools; using these techniques researchers can design new experiments and answer fundamental questions in bioelectronics and fundamental cell biology.

Acknowledgements

The authors are grateful for the continued financial support of the Australian Research Council under the Australian Federation and Laureate Fellowships of Prof Gordon Wallace, the Australian Research Fellowship of Assoc. Prof. Michael Higgins and the QEII Fellowship of Assoc. Prof. Simon Moulton.

Notes and references

[a] ARC Centre of Excellence for Electromaterials Science /Intelligent Polymer Research Institute, Innovation Campus, University of Wollongong, NSW 2522, Australia

1 G. G. Wallace, S. E. Moulton, R. M. I. Kapsa and M. J. Higgins, *Organic Bionics*, Wiley-VCH Verlag GmbH & Co. KGaA, Weinheim, Germany, 2012.

2 G. M. Clark, *Philos. Trans. R. Soc. Lond. B. Biol. Sci.*, 2006, **361**, 791–810.

3 J. S. Perlmutter and J. W. Mink, *Annu. Rev. Neurosci.*, 2006, **29**, 229–57.

4 J. M. Ong and L. da Cruz, *Clin. Experiment. Ophthalmol.*, 2012, **40**, 6–17.
5 J. K. Chapin and K. A. Moxon, Eds., *Neural prostheses for restoration of sensory and motor function. Vol 4.*, CRC Press, 2010.
6 A. L. Velasco, F. Velasco, M. Velasco, D. Trejo, G. Castro and J. D. Carrillo-Ruiz, *Epilepsia*, 2007, **48**, 1895–903.
7 A. A. Al-majed, C. M. Neumann, T. M. Brushart and T. Gordon, 2000, **20**, 2602–2608.
8 T. M. Brushart, P. N. Hoffman, R. M. Royall, B. B. Murinson, C. Witzel and T. Gordon, 2002, **22**, 6631–6638.
9 M. Flaibani, L. Boldrin, E. Cimetta, M. Piccoli, P. De Coppi and N. Elvassore, *Tissue Eng. Part A*, 2009, **15**, 2447–57.
10 N. Tandon, C. Cannizzaro, P.-H. G. Chao, R. Maidhof, A. Marsano, H. T. H. Au, M. Radisic and G. Vunjak-Novakovic, *Nat. Protoc.*, 2009, **4**, 155–73.
11 G. G. Wallace, S. E. Moulton and G. M. Clark, *Science (80-.).*, 2009, **324**, 185–186.
12 B. J. Allitt, S. J. Morgan, S. Bell, D. a X. Nayagam, B. Arhatari, G. M. Clark and a G. Paolini, *Hear. Res.*, 2012, **287**, 30–42.
13 G. W. Gross, E. Rieske, G. W. Kreutzberg and A. Meyer, *Neurosci. Lett.*, 1977, **6**, 101–105.
14 S. F. Cogan, *Annu. Rev. Biomed. Eng.*, 2008, **10**, 275–309.
15 M. J. Higgins, S. T. Mcgovern and G. G. Wallace, *Microscopy*, 2009, 3627–3633.
16 M. M. Stevens and J. H. George, *Science*, 2005, **310**, 1135–8.
17 E. K. F. Yim and K. W. Leong, *Scan. Electron Microsc.*, 2005, **1**, 10 – 21.
18 M. Jonathan, P. Biggs, R. G. Richards and M. J. Dalby, *Nanomedicine Nanotechnology, Biol. Med.*, 2010, **6**, 619–633.
19 S. E. Moulton and G. G. Wallace, *Mater. Aust.*, 2008, 22–23.
20 S. E. Moulton, M. J. Higgins, R. M. I. Kapsa and G. G. Wallace, *Adv. Funct. Mater.*, 2012, **22**, 2003–2014.
21 T. Pan and W. Wang, *Ann. Biomed. Eng.*, 2011, **39**, 600–20.
22 B. D. Gates, Q. Xu, M. Stewart, D. Ryan, C. G. Willson and G. M. Whitesides, *Chem. Rev.*, 2005, **105**, 1171–96.
23 M. Geissler and Y. Xia, *Adv. Mater.*, 2004, **16**, 1249–1269.
24 Y. Wang, C. A. Mirkin and S. Park, 2009, **3**, 1049–1056.
25 D. E. Discher, P. Janmey and Y. Wang, *Science (80-.).*, 2009, **1139**.
26 T. Dvir, B. P. Timko, D. S. Kohane and R. Langer, *Nat. Nanotechnol.*, 2011, **6**, 13–22.
27 R. Langer, *Acc. Chem. Res.*, 2000, **33**, 94–101.
28 R. A. Green, N. H. Lovell, G. G. Wallace and L. A. Poole-warren, *Hear. Res.*, 2008, **29**, 3393–3399.
29 Intel Corporation, *From sand to circuits: How Intel makes integrated circuit chips*, 2008.
30 Semiconductor Industry Association, *International Technology Roadmap for Semiconductors*, Semicoductor Industry Association, 2012.
31 Intel Corportation, *From Sand to Silicon*, 2011.
32 P. Fromherz, *Chemphyschem*, 2002, **3**, 276–84.
33 M. Voelker and P. Fromherz, *Small*, 2005, **1**, 206–10.
34 D. Braeken, R. Huys, J. Loo, C. Bartic, G. Borghs, G. Callewaert and W. Eberle, *Biosens. Bioelectron.*, 2010, **26**, 1474–7.
35 D. Khodagholy, M. Gurfinkel, E. Stavrinidou, P. Leleux, T. Herve, S. Sanaur and G. G. Malliaras, *Appl. Phys. Lett.*, 2011, **99**, 163304.
36 J. A. Defranco, B. S. Schmidt, M. Lipson and G. G. Malliaras, *Org. Electron.*, 2006, **7**, 22–28.
37 S. Y. Yang, B. N. Kim, A. A. Zakhidov, P. G. Taylor, J. Lee, C. K. Ober, M. Lindau and G. G. Malliaras, *Adv. Mater.*, 2011, **23**, H184–8.
38 D. Khodagholy, T. Doublet, P. Quilichini, M. Gurfinkel, P. Leleux, A. Ghestem, E. Ismailova, T. Hervé, S. Sanaur, C. Bernard and G. G. Malliaras, *Nat. Commun.*, 2013, **4**, 1575.
39 S. Mary, E. Merriam, S. Dehmel, O. Srivannavit, S. E. Shore, K. D. Wise and L. Fellow, 2011, **58**, 397–403.
40 Q. Bai and K. D. Wise, *IEEE Trans. Biomed. Eng.*, 2001, **48**, 911–920.
41 F. Patolsky, B. P. Timko, G. Yu, Y. Fang, A. B. Greytak, G. Zheng and C. M. Lieber, *Science*, 2006, **313**, 1100–4.
42 A. Kumar, H. a. Biebuyck and G. M. Whitesides, *Langmuir*, 1994, **10**, 1498–1511.
43 S. Monolayers, B. J. L. Wilbur, A. Kumar, E. Kim and G. M. Whitesides, 1994, 600–604.
44 H. Li, B. V. O. Muir, G. Fichet and W. T. S. Huck, *Langmuir*, 2003, **19**, 1963–1965.
45 E. Ostuni, G. M. Whitesides, D. E. Ingber and C. S. Chen, *Methods Mol. Biol.*, 2009, **522**, 183–94.
46 J. L. Tan, J. Tien, D. M. Pirone, D. S. Gray, K. Bhadriraju and C. S. Chen, 2002, **2002**.
47 D. B. Weibel, W. R. Diluzio and G. M. Whitesides, *Nat. Rev. Microbiol.*, 2007, **5**, 209–18.
48 D. Lehnert, B. Wehrle-Haller, C. David, U. Weiland, C. Ballestrem, B. a Imhof and M. Bastmeyer, *J. Cell Sci.*, 2004, **117**, 41–52.
49 J.-U. Park, M. Hardy, S. J. Kang, K. Barton, K. Adair, D. K. Mukhopadhyay, C. Y. Lee, M. S. Strano, A. G. Alleyne, J. G. Georgiadis, P. M. Ferreira and J. a Rogers, *Nat. Mater.*, 2007, **6**, 782–9.
50 P. Calvert, *Chem. Mater.*, 2001, **13**, 3299–3305.
51 P. Calvert, *Science*, 2007, **318**, 208–9.
52 C. J. Ferris, K. J. Gilmore, S. Beirne, D. McCallum, G. G. Wallace and M. in het Panhuis, *Biomater. Sci.*, 2013, **1**, 224.
53 J. a Rogers and U. Paik, *Nat. Nanotechnol.*, 2010, **5**, 385–6.
54 D. M. Eigler and E. K. Schweizer, *Nature*, 1990, **344**, 524–526.
55 M. Fuechsle, J. a Miwa, S. Mahapatra, H. Ryu, S. Lee, O. Warschkow, L. C. L. Hollenberg, G. Klimeck and M. Y. Simmons, *Nat. Nanotechnol.*, 2012, **7**, 242–6.
56 X. Li, P. Nardi, C.-W. Baek, J.-M. Kim and Y.-K. Kim, *J. Micromechanics Microengineering*, 2005, **15**, 551–556.
57 H. W. Schumacher, U. F. Keyser, U. Zeitler, R. J. Haug and K. Eberl, *Appl. Phys. Lett.*, 1999, **75**, 1107.
58 P. M. Campbell, E. S. Snow and P. J. McMarr, *Appl. Phys. Lett.*, 1995, **66**, 1388.
59 E. S. Snow and P. M. Campbell, *Appl. Phys. Lett.*, 1994, **64**, 1932.
60 O. Loh, R. Lam, M. Chen, N. Moldovan, H. Huang, D. Ho and H. D. Espinosa, *Small*, 2009, **5**, 1667–74.
61 R. Garcia, A. W. Knoll and E. Riedo, *Nat. Nanotechnol.*, 2014, **9**, 577–87.
62 G. K. Binnig, 2000, **44**, 323–340.
63 P. Vettiger, M. Despont, U. Drechsler, U. Durig, W. Haberle, M. I. Lutwyche, H. E. Rothuizen, R. Stutz, R. Widmer and G. K. Binnig, *IBM J. Res. Dev.*, 2000, **44**, 323–340.
64 S. Xu and G. Liu, *Langmuir*, 1997, **13**, 127–129.
65 C. Staii, D. W. Wood and G. Scoles, *J. Am. Chem. Soc.*, 2008, **130**, 640–6.
66 J. C. Garno, Y. Yang, N. a. Amro, S. Cruchon-Dupeyrat, S. Chen and G.-Y. Liu, *Nano Lett.*, 2003, **3**, 389–395.
67 A. Fuhrer, S. Lüscher, T. Ihn, T. Heinzel, K. Ensslin, W. Wegscheider and M. Bichler, *Nature*, 2001, **413**, 822–5.
68 S. C. Minne, J. D. Adams, G. Yaralioglu, S. R. Manalis, A. Atalar and C. F. Quate, *Appl. Phys. Lett.*, 1998, **73**, 1742.
69 K. Salaita, Y. Wang and C. A. Mirkin, *Nat. Nanotechnol.*, 2007, **2**, 145–55.
70 K. Kim, N. Moldovan and H. D. Espinosa, *Small*, 2005, **1**, 632–5.
71 N. Moldovan, K.-H. Kim and H. D. Espinosa, *J. Microelectromechanical Syst.*, 2006, **15**, 204–213.
72 a. Meister, M. Liley, J. Brugger, R. Pugin and H. Heinzelmann, *Appl. Phys. Lett.*, 2004, **85**, 6260.
73 B. Wu, A. Ho, N. Moldovan and H. D. Espinosa, *Langmuir*, 2007, **23**, 9120–3.
74 K.-H. Kim, R. G. Sanedrin, A. M. Ho, S. W. Lee, N. Moldovan, C. A. Mirkin and H. D. Espinosa, *Adv. Mater.*, 2008, **20**, 330–334.
75 O. Y. Loh, A. M. Ho, J. E. Rim, P. Kohli, N. a Patankar and H. D. Espinosa, *Proc. Natl. Acad. Sci. U. S. A.*, 2008, **105**, 16438–43.
76 C. Laslau, D. E. Williams and J. Travas-Sejdic, *Prog. Polym. Sci.*, 2012, **37**, 1177–1191.
77 J. Hu and M.-F. Yu, *Science*, 2010, **329**, 313–6.
78 G.-Y. Liu, S. Xu and Y. Qian, *Acc. Chem. Res.*, 2000, **33**, 457–466.
79 R. Garcia, R. V Martinez and J. Martinez, *Chem. Soc. Rev.*, 2006, **35**, 29–38.
80 R. D. Piner, *Science (80-.).*, 1999, **283**, 661–663.
81 Y. Li, B. W. Maynor and J. Liu, *J. Am. Chem. Soc.*, 2001, **123**, 2105–2106.

82 B. a. Nelson, W. P. King, a. R. Laracuente, P. E. Sheehan and L. J. Whitman, *Appl. Phys. Lett.*, 2006, **88**, 033104.
83 D. A. Weinberger, S. Hong, C. A. Mirkin, B. W. Wessels and T. B. Higgins, *Adv. Mater.*, 2000, **12**, 1600–1603.
84 H. Wang, O. A. Nafday, J. R. Haaheim, E. Tevaarwerk, N. A. Amro, R. G. Sanedrin, C. Chang, F. Ren and S. J. Pearton, *Appl. Phys. Lett.*, 2008, **93**, 143105.
85 S. Hung, O. A. Nafday, J. R. Haaheim, F. Ren, G. C. Chi and S. J. Pearton, *J. Phys. Chem. C*, 2010, **114**, 9672–9677.
86 A. Hernandez-Santana, E. Irvine, K. Faulds and D. Graham, *Chem. Sci.*, 2011, **2**, 211.
87 B. W. Maynor, S. F. Filocamo, M. W. Grinstaff and J. Liu, *J. Am. Chem. Soc.*, 2002, **124**, 522–523.
88 M. Su, M. Aslam, L. Fu, N. Wu and V. P. Dravid, *Appl. Phys. Lett.*, 2004, **84**, 4200.
89 J.-H. Lim and C. A. Mirkin, *Adv. Mater.*, 2002, **14**, 1474–1477.
90 J.-H. Lim, D. S. Ginger, K.-B. Lee, J. Heo, J.-M. Nam and C. a Mirkin, *Angew. Chem. Int. Ed. Engl.*, 2003, **42**, 2309–12.
91 A. J. Senesi, D. I. Rozkiewicz, D. N. Reinhoudt and C. A. Mirkin, *ACS Nano*, 2009, **3**, 2394–402.
92 J.-W. Jang, A. Smetana and P. Stiles, *Scanning*, 2010, **32**, 24–9.
93 H. Nakashima, M. J. Higgins, C. O'Connell, K. Torimitsu and G. G. Wallace, *Langmuir*, 2012, **28**, 804–11.
94 R. Sistiabudi and A. Ivanisevic, *Adv. Mater.*, 2008, **20**, 3678–3681.
95 K. Salaita, Y. Wang, J. Fragala, R. a Vega, C. Liu and C. a Mirkin, *Angew. Chem. Int. Ed. Engl.*, 2006, **45**, 7220–3.
96 F. Huo, Z. Zheng, G. Zheng, L. R. Giam, H. Zhang and C. A. Mirkin, *Science*, 2008, **321**, 1658–60.
97 D. K. Hoover, E. Lee, E. W. L. Chan and M. N. Yousaf, *Chembiochem*, 2007, **8**, 1920–3.
98 D. K. Hoover, E. W. L. Chan and M. N. Yousaf, *J. Am. Chem. Soc.*, 2008, **130**, 3280–1.
99 J. M. Curran, R. Stokes, E. Irvine, D. Graham, N. a Amro, R. G. Sanedrin, H. Jamil and J. a Hunt, *Lab Chip*, 2010, **10**, 1662–70.
100 J. M. Curran, R. Chen, R. Stokes, E. Irvine, D. Graham, E. Gubbins, D. Delaney, N. Amro, R. Sanedrin, H. Jamil and J. a Hunt, *J. Mater. Sci. Mater. Med.*, 2010, **21**, 1021–9.
101 L. R. Giam, M. D. Massich, L. Hao, L. Shin Wong, C. C. Mader and C. A. Mirkin, *Proc. Natl. Acad. Sci. U. S. A.*, 2012, **109**, 1–6.
102 P. L. Stiles, *Nat. Publ. Gr.*, 2010, **7**, i–ii.
103 C. D. O'Connell, M. J. Higgins, D. Marusic, S. E. Moulton and G. G. Wallace, *Langmuir*, 2014, **30**, 2712–21.
104 C. D. O'Connell, M. J. Higgins, R. P. Sullivan, S. E. Moulton and G. G. Wallace, *Small*, 2014, **10**, 3717–28.
105 M. Ben Ali, T. Ondarc, M. Brust and C. Joachim, 2002, 872–876.
106 M. Wiechmann, O. Enders, F. Leisten, J. M. Becker, R. J. Haug and H. Kolb, *Surf. Interface Anal.*, 2006, **38**, 1004–1009.
107 W. M. Wang, R. M. Stoltenberg, S. Liu and Z. Bao, *ACS Nano*, 2008, **2**, 2135–42.
108 B. W. Maynor, Y. Li and J. Liu, *Langmuir*, 2001, **17**, 2575–2578.
109 L. a. Porter, H. C. Choi, J. M. Schmeltzer, A. E. Ribbe, L. C. C. Elliott and J. M. Buriak, *Nano Lett.*, 2002, **2**, 1369–1372.
110 Y. Cai and B. M. Ocko, *J. Am. Chem. Soc.*, 2005, **127**, 16287–91.
111 R. J. Barsotti, Jr. and F. Stellacci, *J. Mater. Chem.*, 2006, **16**, 962.
112 H. Zhang, R. Jin and C. A. Mirkin, *Nano Lett.*, 2004, **4**, 1493–1495.
113 K. S. Salaita, S. W. Lee, D. S. Ginger and C. a Mirkin, *Nano Lett.*, 2006, **6**, 2493–8.
114 W.-K. Lee, S. Chen, A. Chilkoti and S. Zauscher, *Small*, 2007, **3**, 249–54.
115 B. Basnar, Y. Weizmann, Z. Cheglakov and I. Willner, *Adv. Mater.*, 2006, **18**, 713–718.
116 J. Chai, F. Huo, Z. Zheng, L. R. Giam, W. Shim and C. A. Mirkin, *Proc. Natl. Acad. Sci. U. S. A.*, 2010, **107**, 20202–6.
117 M. G. Sung, T.-Y. Lee, B. Kim, T. H. Kim and S. Hong, *Langmuir*, 2010, **26**, 1507–11.
118 J.-W. Jang, R. G. Sanedrin, A. J. Senesi, Z. Zheng, X. Chen, S. Hwang, L. Huang and C. a Mirkin, *Small*, 2009, **5**, 1850–3.
119 H. Zhang and C. A. Mirkin, *Chem. Mater.*, 2004, **16**, 1480–1484.
120 C. D. O'Connell, M. J. Higgins, R. P. Sullivan, S. S. Jamali, S. E. Moulton and G. G. Wallace, *Nanotechnology*, 2013, **24**, 505301.
121 D. J. Pena, M. P. Raphael and J. M. Byers, *Society*, 2003, 9028–9032.
122 W. M. Wang, N. Stander, R. M. Stoltenberg, D. Goldhaber-Gordon and Z. Bao, *ACS Nano*, 2010, **4**, 6409–16.
123 C. A. Mirkin, *ACS Nano*, 2007, **1**, 79–83.
124 H.-H. Lu, C.-Y. Lin, T.-C. Hsiao, Y.-Y. Fang, K.-C. Ho, D. Yang, C.-K. Lee, S.-M. Hsu and C.-W. Lin, *Anal. Chim. Acta*, 2009, **640**, 68–74.
125 C. D. O'Connell, M. J. Higgins, H. Nakashima, S. E. Moulton and G. G. Wallace, *Langmuir*, 2012, **28**, 9953–60.
126 M. Wagner, C. D. O'Connell, D. G. Harman, R. Sullivan, A. Ivaska, M. J. Higgins and G. G. Wallace, *Synth. Met.*, 2013, **181**, 64–71.
127 B. J. Lim and C. A. Mirkin, 2010, 1474–1477.
128 L. M. Demers, D. S. Ginger, S.-J. Park, Z. Li, S.-W. Chung and C. A. Mirkin, *Science*, 2002, **296**, 1836–8.
129 D. L. Wilson, R. Martin, S. Hong, M. Cronin-Golomb, C. a Mirkin and D. L. Kaplan, *Proc. Natl. Acad. Sci. U. S. A.*, 2001, **98**, 13660–4.
130 R. a Vega, D. Maspoch, K. Salaita and C. a Mirkin, *Angew. Chem. Int. Ed. Engl.*, 2005, **44**, 6013–5.
131 J. Kim, Y.-H. Shin, S.-H. Yun, D.-S. Choi, J.-H. Nam, S. R. Kim, S.-K. Moon, B. H. Chung, J.-H. Lee, J.-H. Kim, K.-Y. Kim, K.-M. Kim and J.-H. Lim, *J. Am. Chem. Soc.*, 2012, **134**, 16500–3.
132 C.-C. Wu, D. N. Reinhoudt, C. Otto, V. Subramaniam and A. H. Velders, *Small*, 2011, **7**, 989–1002.
133 K.-B. Lee, E.-Y. Kim, C. a. Mirkin and S. M. Wolinsky, *Nano Lett.*, 2004, **4**, 1869–1872.
134 M. Lee, H.-K. Yang, K.-H. Park, D.-K. Kang, S.-I. Chang and I.-C. Kang, *Biochem. Biophys. Res. Commun.*, 2007, **362**, 935–9.
135 J. Chai, L. S. Wong, L. Giam and C. a Mirkin, *Proc. Natl. Acad. Sci. U. S. A.*, 2011, **108**, 19521–5.
136 R. a Vega, C. K.-F. Shen, D. Maspoch, J. G. Robach, R. a Lamb and C. a Mirkin, *Small*, 2007, **3**, 1482–5.
137 J. P. Vacanti and R. Langer, *Lancet*, 1999, **354**, S32–S34.
138 M. N. Yousaf, *Curr. Opin. Chem. Biol.*, 2009, **13**, 697–704.
139 M. Mrksich, *Chem. Soc. Rev.*, 2000, **29**, 267–273.
140 C. S. Chen, M. Mrksich, S. Huang, G. M. Whitesides and D. E. Ingber, *Science (80-.).*, 1997, **276**, 1425–1428.
141 K.-B. Lee, S.-J. Park, C. a Mirkin, J. C. Smith and M. Mrksich, *Science*, 2002, **295**, 1702–5.
142 J. M. Collins and S. Nettikadan, *Anal. Biochem.*, 2011, **419**, 339–41.
143 S. Sekula, J. Fuchs, S. Weg-Remers, P. Nagel, S. Schuppler, J. Fragala, N. Theilacker, M. Franzreb, C. Wingren, P. Ellmark, C. a K. Borrebaeck, C. a Mirkin, H. Fuchs and S. Lenhert, *Small*, 2008, **4**, 1785–93.
144 Y. Narui and K. S. Salaita, *Chem. Sci.*, 2012, **3**, 794.
145 J. M. Collins, R. T. S. Lam, Z. Yang, B. Semsarieh, A. B. Smetana and S. Nettikadan, *Lab Chip*, 2012, **12**, 2643–8.
146 Z. Zheng, W. L. Daniel, L. R. Giam, F. Huo, A. J. Senesi, G. Zheng and C. A. Mirkin, *Angew. Chemie*, 2009, **121**, 7762–7765.
147 M. Zhang, D. Bullen, S. Chung, S. Hong, K. S. Ryu, Z. Fan, C. A. Mirkin and C. Liu, *Nanotechnology*, 2002, **13**, 212–217.
148 J. R. Haaheim, E. R. Tevaarwerk, J. Fragala and R. Shile, eds. T. George and Z. Cheng, 2008, vol. 6959, p. 69590I–69590I–11.
149 A. B. Braunschweig, F. Huo and C. a Mirkin, *Nat. Chem.*, 2009, **1**, 353–8.
150 X. Liao, A. B. Braunschweig and C. a Mirkin, *Nano Lett.*, 2010, **10**, 1335–40.
151 X. Liao, A. B. Braunschweig, Z. Zheng and C. a Mirkin, *Small*, 2010, **6**, 1082–6.
152 W. Shim, A. B. Braunschweig, X. Liao, J. Chai, J. K. Lim, G. Zheng and C. a Mirkin, *Nature*, 2011, **469**, 516–20.
153 F. Huo, G. Zheng, X. Liao, L. R. Giam, J. Chai, X. Chen, W. Shim and C. A. Mirkin, *Nat. Nanotechnol.*, 2010, **5**, 637–40.
154 D. Bullen, S.-W. Chung, X. Wang, J. Zou, C. a. Mirkin and C. Liu, *Appl. Phys. Lett.*, 2004, **84**, 789.
155 D. Bullen and C. Liu, *Sensors Actuators A Phys.*, 2006, **125**, 504–511.
156 B. C. Thompson, S. E. Moulton, J. Ding, R. Richardson, A. Cameron, S. O. Leary, G. G. Wallace and G. M. Clark, *J. Control. Release*, 2006, **116**, 285 – 294.
157 T. E. Campbell, a. J. Hodgson and G. G. Wallace, *Electroanalysis*, 1999, **11**, 215–222.